

Neutrino pair emission due to scattering of electrons off fluxoids in superfluid neutron star cores

A.D. Kaminker¹, D.G. Yakovlev¹, and P. Haensel²

¹ A.F. Ioffe Institute of Physics and Technology, 194021 St. Petersburg, Russia

² N. Copernicus Astronomical Center, Polish Academy of Sciences, Bartycka 18, PL-00716 Warszawa, Poland

Received 25 November 1996 / Accepted 29 January 1997

Abstract. We study the emission of neutrinos, resulting from the scattering of electrons off magnetic flux tubes (fluxoids) in the neutron star cores with superfluid (superconducting) protons. In the absence of proton superfluidity ($T \geq T_{cp}$), this process transforms into the well known electron synchrotron emission of neutrino pairs in a locally uniform magnetic field B , with the neutrino energy loss rate Q proportional to $B^2 T^5$. For temperatures T not much below T_{cp} , the synchrotron regime ($Q \propto T^5$) persists and the emissivity Q can be amplified by several orders of magnitude due to the appearance of the fluxoids and associated enhancement of the field within them. For lower T , the synchrotron regime transforms into the bremsstrahlung regime ($Q \propto T^6$) similar to the ordinary neutrino-pair bremsstrahlung of electrons which scatter off atomic nuclei. We calculate Q numerically and represent our results through a suitable analytic fit. In addition, we estimate the emissivities of two other neutrino-production mechanisms which are usually neglected – neutrino-pair bremsstrahlung processes due to electron-proton and electron-electron collisions. We show that the electron-fluxoid and electron-electron scattering can provide the main neutrino production mechanisms in the neutron star cores with highly superfluid protons and neutrons at $T \lesssim 5 \times 10^8$ K. The electron-fluxoid scattering is significant if the initial, locally uniform magnetic field $B \gtrsim 10^{13}$ G.

Key words: dense matter – stars: interiors – stars: neutron

1. Introduction

Neutrino energy losses play a decisive role in cooling of young neutron stars (NSs). During first $10^5 - 10^6$ yrs after the NS birth, the cooling is dominated by the neutrino emission from the NS cores, of density exceeding the normal nuclear matter density, $\rho_0 = 2.7 \times 10^{14}$ g cm⁻³ (corresponding to the nucleon number density $n_0 = 0.16$ fm⁻³).

Send offprint requests to: P. Haensel

The emission of neutrinos results from the weak interaction processes involving baryons and/or leptons in the NS cores. The presence of the strong internal magnetic field allows an additional process — the neutrino synchrotron radiation of electrons. This process was considered by many authors (e.g. Kaminker et al. 1991, 1992, and references therein) for a spatially homogeneous magnetic field.

It is widely accepted (see, e.g., Takatsuka & Tamagaki 1993, and references therein), that neutrons and/or protons in the NS core can be superfluid. Let T_{cp} and T_{cn} be the critical temperatures of the proton and neutron superfluidities, respectively. Theoretical values of T_{cp} and T_{cn} are strongly model dependent and range from 10^8 to 10^{10} K. For $T \ll T_c$, the superfluidity of nucleons strongly suppresses the neutrino luminosity produced by the Urca and bremsstrahlung processes in the NS cores (e.g., Pethick 1992, Yakovlev & Levenfish 1995). This enhances the relative importance of the neutrino synchrotron process.

It is commonly thought that superfluid protons form the type II superconductor (see Sauls 1989, and references therein). Let us assume that the core of a newly born, hot and initially non-superfluid NS contains a magnetic field (e.g., primordial one, or generated at the NS formation stage). The transition to a superconducting state in the course of the stellar cooling would then be accompanied by a dramatic change in the spatial structure of the magnetic field. Initially homogeneous field splits into an ensemble of fluxoids which contain a superstrong magnetic field, embedded in the field-free superconducting medium. So far, the neutrino synchrotron radiation has been studied only for a homogeneous magnetic field. In the present paper, we show that after the superfluidity onset, the neutrino synchrotron mechanism transforms into the neutrino pair emission due to the electron-fluxoid scattering.

Physical conditions in the superconducting NS cores are described in Sect. 2. In Sect. 3, we present general formalism of the electron-fluxoid (*ef*) scattering. The calculations of the neutrino emissivity are performed in Sect. 4. In Sect. 5, we estimate the emissivities of two additional neutrino production mechanisms which are usually neglected: the bremsstrahlung processes due to electron-proton (*ep*) and electron-electron (*ee*)

scattering. No calculation of these emissivities has been done earlier, to our knowledge, although the importance of the ep scattering has been mentioned by Schaab et al. (1996). In Sect. 6 we show that the new mechanisms (especially ef and ee scattering) can be important in the NS cores with highly superfluid protons and neutrons since the superfluidity reduces strongly the familiar neutrino generation reactions (Urca processes, nucleon-nucleon bremsstrahlung).

2. Superconducting neutron star cores

The density within a NS core is expected to range from about $0.5\rho_0$ at its outer edge (Lorenz et al. 1993), to $(5-10)\rho_0$ at the star center. For densities $\rho \lesssim 2\rho_0$, matter consists of neutrons, with a few percent admixture of protons, electrons, and possibly muons. The fraction of muons is usually much smaller than that of electrons, and a simple npe model is a good approximation. At higher densities, $\rho \gtrsim 2\rho_0$, other particles may appear, such as hyperons, condensed pions and/or kaons, or even free quarks. Dependence of the neutrino emissivity on the composition of dense matter is reviewed by Pethick (1992). For simplicity, we will neglect exotic matter constituents, restricting ourselves to the simplest npe model. All constituents of the npe matter are degenerate. The electrons form an ultrarelativistic and almost ideal gas, with the electron Fermi energy $\mu_e \approx \hbar c(3\pi^2 n_e)^{1/3} \sim (100-300)$ MeV, where n_e is the electron number density. The neutrons and protons form strongly interacting Fermi liquids. The Fermi energy of neutrons is of the order of that of the electrons, while the Fermi energy of protons is much smaller.

Both nucleon species, n and p , can be in a superfluid state (for a review, see Takatsuka & Tamagaki 1993). The superfluidity is widely accepted to be of the BCS-type; the nn and/or pp pairing occurs due to nuclear attraction. Let us focus on the proton superfluidity. In view of a relatively low proton number density, the inter-proton distance is rather high, and the pp interaction is attractive in the 1S_0 state. Thus, the proton pairing is most likely to be in the 1S_0 state. Recent reviews on the properties of superconducting protons in the NS cores are given by Sauls (1989) and Bhattacharya & Srinivasan (1995). The proton superconductivity is characterized by an isotropic energy gap in the single-(quasi)particle spectrum Δ_p , which depends on temperature and density. The critical temperature T_{cp} is related to the zero-temperature energy gap $\Delta_p(0)$ by $T_{cp} = \Delta_p(0)/(1.76 k_B)$ (Lifshitz & Pitaevskii 1980), where k_B is the Boltzmann constant. An important parameter of superconducting protons is the pp correlation length ξ ; it measures the size of a pp Cooper pair. In the BCS model, ξ is related to Δ_p and the proton Fermi velocity v_{Fp} by $\xi = \hbar v_{Fp}/(\pi \Delta_p)$. The zero temperature value of ξ will be denoted by ξ_0 . Another important parameter is the penetration depth λ of the magnetic field into a proton superconductor. In the case of $\lambda \gg \xi$ (which corresponds to the conditions prevailing in the NS cores), the

zero temperature penetration depth, λ_0 , is determined by the proton plasma frequency, ω_p (e.g., Lifshitz & Pitaevskii 1980),

$$\lambda_0 = \frac{c}{\omega_p}, \quad \omega_p = \left(\frac{4\pi n_p e^2}{m_p^*} \right)^{1/2}, \quad (1)$$

where n_p is the proton number density, and m_p^* is the proton effective mass, that can differ from the bare mass m_p due to the many-body effects in dense matter. Simple estimates yield typical values of ξ_0 of a few fm, and λ_0 of a few ten fm. If so, $\lambda_0 \gg \xi_0$, which means that protons constitute a type II superconductor. Notice that the values of λ_0 and ξ_0 are model dependent, and one cannot exclude the case of $\lambda_0 \sim \xi_0$, in which the proton superconductivity could be of type I, although we will not consider this case in the present article (some comments on the case of a type I proton superconductor are given at the end of Sect. 6).

For $T \rightarrow T_{cp}$, both ξ and λ diverge as $(T_{cp} - T)^{-1/2}$, while for $T \ll T_{cp}$ they can be replaced by their zero temperature values, ξ_0 and λ_0 . However, we need to know the temperature dependence of λ for all temperatures below T_{cp} . In what follows, we will approximate its temperature dependence by the Gorter-Casimir formula (Tilley & Tilley 1990),

$$\lambda = \frac{\lambda_0}{\sqrt{1 - (T/T_{cp})^4}}. \quad (2)$$

The transition to the type II superconductivity during the NS cooling is accompanied by the formation of quantized flux tubes (Abrikosov fluxoids), parallel to the initial local magnetic field \vec{B} . Each fluxoid carries an elementary magnetic flux $\phi_0 = \pi \hbar c/e$. The number of fluxoids per unit area perpendicular to the initial field is $\mathcal{N}_F = \bar{B}/\phi_0$, and the mean distance between the fluxoids is $d_F = [2\phi_0/(\sqrt{3}\bar{B})]^{1/2}$. Simple estimate yields $d_F \approx 1500/(\bar{B}_{13})^{1/2}$ fm, where $\bar{B}_{13} \equiv \bar{B}/(10^{13} \text{ G})$. A fluxoid has a small central core of radius $\sim \xi$ containing normal protons. A typical fluxoid radius is λ . Just after the superconductivity onset ($T < T_{cp}$), this radius is large and the fluxoids fill all the available space. When temperature drops to about $0.8T_{cp}$, λ reduces nearly to its zero-temperature value λ_0 . Thus, λ becomes much smaller than the inter-fluxoid distance d_F , for the magnetic fields $\bar{B} < 10^{15}$ G which we will consider in the present article. The maximum value of B is reached at the fluxoid axis, $B_{\max} \simeq [\phi_0/(\pi\lambda^2)] \log(\lambda/\xi)$. In our case $\lambda \gg \xi$, and the magnetic field profile at $r \gg \xi$ is given by (e.g., Lifshitz & Pitaevskii 1980):

$$B(r) = \frac{\phi_0}{2\pi\lambda^2} K_0\left(\frac{r}{\lambda}\right), \quad (3)$$

where $K_0(x)$ is a McDonald function. In particular, for $r \gg \lambda$, one has $B(r) \approx \phi_0(8\pi r\lambda^3)^{-1/2} \exp(-r/\lambda)$.

The superconducting state is destroyed when $d_F < \xi$, which corresponds to magnetic fields $\bar{B} > B_{c2} = \phi_0/(\pi\xi^2)$, whose typical values are $\sim 10^{18}$ G. We do not consider such strong fields.

Let us mention that the fluxoids may migrate slowly outward the stellar core due to the buoyancy forces (Muslimov & Tsygan 1985, Jones 1987, Srinivasan et al. 1990).

3. General formalism

Consider the neutrino-pair emission due to scattering of strongly degenerate, relativistic electrons off fluxoids (Sect. 2),

$$e + f \rightarrow e + f + \nu + \bar{\nu}. \quad (4)$$

We will treat this process using the standard perturbation theory with free electrons in nonperturbed states. The process (4) is similar to the well known neutrino-pair bremsstrahlung due to scattering of electrons by atomic nuclei (see, e.g., Festa and Ruderman 1969, Soyeur and Brown 1979, Haensel et al. 1996, and references therein). It is described by two second-order diagrams, where one (electromagnetic) vertex is associated with electron scattering by the fluxoid magnetic fields, while the other (four-tail) vertex is due to the neutrino-pair emission.

In what follows, we will mainly use the units in which $c = \hbar = k_B = 1$ although we will insert the ordinary physical units in the final expressions.

The neutrino energy loss rate (emissivity) Q_{flux} (ergs cm⁻³ s⁻¹) of process (4) can be written as

$$Q_{\text{flux}} = \frac{\mathcal{A}_F}{(2\pi)^{10}} \int d\mathbf{p} \int d\mathbf{p}' \int d\mathbf{k}_\nu \int d\mathbf{k}'_\nu \times \delta(\varepsilon - \varepsilon' - \omega) \delta(p_z - p'_z - k_z) \omega f(1 - f') W, \quad (5)$$

where \mathcal{A}_F is the fluxoid surface number density defined in Sect. 2, $P = (\varepsilon, \mathbf{p})$ and $P' = (\varepsilon', \mathbf{p}')$ are, respectively, the electron 4-momenta in the initial and final states, $K_\nu = (\omega_\nu, \mathbf{k}_\nu)$ and $K'_\nu = (\omega'_\nu, \mathbf{k}'_\nu)$ are the 4-momenta of the neutrino and of the antineutrino, and $K = K_\nu + K'_\nu = (\omega, \mathbf{k})$ is the 4-momentum of the neutrino pair ($\omega = \omega_\nu + \omega'_\nu$ and $\mathbf{k} = \mathbf{k}_\nu + \mathbf{k}'_\nu$). Furthermore,

$$f = \left[1 + \exp\left(\frac{\varepsilon - \mu}{T}\right) \right]^{-1} \quad (6)$$

is the Fermi-Dirac function for the initial electron state, and $f' \equiv f(\varepsilon')$ is the same function for the final electron state. The δ -functions describe energy conservation and momentum conservation along the fluxoid axis (the axis z). Finally, W is the differential transition rate

$$W = \frac{G_F^2}{2} \frac{1}{(2\omega_\nu)(2\omega'_\nu)(2\varepsilon)(2\varepsilon')} \sum_{\sigma, \nu} |M|^2, \quad (7)$$

where $G_F = 1.436 \times 10^{-49}$ erg cm³ is the Fermi weak interaction constant, and $|M|^2$ is the squared transition matrix element. Summation is over the electron spin states σ before and after scattering and over the neutrino flavors (ν_e, ν_μ, ν_τ). The neutrino energies are assumed to be much lower than the intermediate boson mass (~ 80 GeV). Then the standard approach yields

$$\begin{aligned} \sum_{\sigma} |M|^2 &= e^2 \int d\mathbf{q} \delta(\mathbf{p} - \mathbf{q} - \mathbf{p}' - \mathbf{k}) A^i A^{j*} \\ &\times \text{Tr}(\hat{K}_\nu O^\alpha \hat{K}'_\nu O^\beta) \\ &\times \text{Tr}[\bar{L}_{\beta j}(\hat{P}' + m_e) L_{\alpha i}(\hat{P} + m_e)], \quad (8) \\ O^\alpha &= \gamma^\alpha (1 + \gamma^5), \end{aligned}$$

$$L_{\alpha i} = \Gamma_\alpha G(P - Q) \gamma_i + \gamma_i G(P' + Q) \Gamma_\alpha, \quad (9)$$

$$G(P) = \frac{\hat{P} + m_e}{P^2 - m_e^2}, \quad \Gamma^\alpha = C_V \gamma^\alpha + C_A \gamma^\alpha \gamma^5. \quad (10)$$

Here, $\mathbf{q} = \mathbf{p} - \mathbf{p}' - \mathbf{k}$ is a momentum transfer (in the (x, y) -plane) from an electron to a fluxoid, $Q = P - P' - K = (\Omega, \mathbf{q})$ is an appropriate 4-momentum transfer (with no energy transfer, $\Omega = 0$), $\mathbf{A} \equiv \mathbf{A}(\mathbf{q})$ is a 2-dimensional Fourier transform of the magnetic-field vector-potential, which lies in the (x, y) plane, and m_e is the electron mass. Greek indices α and β run over (0,1,2,3) and Latin ones i and j refer to the spatial components (1,2,3); $G(P)$ is the free-electron propagator, γ^α is a Dirac matrix, upper bar denotes Dirac conjugate, and $\hat{P} \equiv P_\alpha \gamma^\alpha$ (Berestetskii et al. 1982). Furthermore, C_V and C_A are the vector and the axial vector weak interaction constants, respectively. For the emission of the electron neutrinos (charged + neutral currents), one has $C_V = 2 \sin^2 \theta_W + 0.5$ and $C_A = 0.5$, while for the emission of the muonic or the tauonic neutrinos (neutral currents only), $C'_V = 2 \sin^2 \theta_W - 0.5$ and $C'_A = -0.5$; θ_W is the Weinberg angle, $\sin^2 \theta_W \simeq 0.23$.

Using the identity (Berestetskii et al. 1982)

$$\begin{aligned} &\int d\mathbf{k}_\nu \int d\mathbf{k}'_\nu \delta^{(4)}(K - K_\nu - K'_\nu) \frac{K_\nu^\alpha K'^\beta_\nu}{\omega_\nu \omega'_\nu} \\ &= \frac{\pi}{6} (K^2 g^{\alpha\beta} + 2K^\alpha K^\beta), \quad (11) \end{aligned}$$

we obtain

$$\begin{aligned} Q_{\text{flux}} &= \frac{e^2 G_F^2 \mathcal{A}_F}{12(2\pi)^9} \int d\mathbf{p} \int d\mathbf{p}' \int d\mathbf{k} \delta(p_z - p'_z - k_z) \\ &\times A^i A^{j*} \frac{\omega}{\varepsilon \varepsilon'} J_{ij} f(1 - f'), \quad (12) \end{aligned}$$

$$\begin{aligned} J_{ij} &= \sum_{\nu} (K^\alpha K^\beta - K^2 g^{\alpha\beta}) \\ &\times \text{Tr}[(\hat{P}' + m_e) L_{\alpha i} (\hat{P} + m_e) \bar{L}_{\beta j}], \quad (13) \end{aligned}$$

where $g^{\alpha\beta} = \text{diag}(1, -1, -1, -1)$ is the metric tensor. The integration in Eq. (12) is to be carried out over the domain in which $K^2 \geq 0$. Notice that Eq. (12) reproduces the well-known expression for the neutrino-pair bremsstrahlung of electrons which scatter off atomic nuclei (e.g., Haensel et al. 1996). For this purpose, one needs only to replace $2\pi \mathcal{A}_F e^2 \delta(p_z - p'_z - k_z) A^i A^{j*} \rightarrow n_i |U(\mathbf{q})|^2 \delta_{ij} \delta_{i0}$, where n_i is the number density of nuclei and $U(\mathbf{q})$ is the Fourier transform of the electron-nucleus Coulomb potential.

The 2-dimensional Fourier transform $B(q) = B_z(q)$ of the fluxoid magnetic field (3) in cylindrical coordinates is

$$B(q) = \frac{\Phi_0}{\lambda^2} \int_0^\infty dr r K_0\left(\frac{r}{\lambda}\right) J_0(qr) \frac{\Phi_0 q_0^2}{q^2 + q_0^2}, \quad (14)$$

where $J_0(x)$ is a Bessel function and $q_0 = 1/\lambda$. Then, using cylindrical gauge, we have $\mathbf{A}(\mathbf{q}) = -i \mathbf{e}_A B(q)/q$, $\mathbf{e}_A = (\mathbf{B} \times \mathbf{q})/(Bq)$ being a unit vector. Accordingly, in Eq. (12) $A^i A^{j*} = (B(q)/q)^2 e_A^i e_A^j$, where $i, j = 1$ or 2 , for nonvanishing components.

Eqs. (12) and (13) determine the neutrino emissivity for any degree of electron degeneracy and relativism. We are interested in the case of ultrarelativistic, strongly degenerate electrons (Sect. 2). In the relativistic limit, tedious but straightforward calculations yield:

$$e_A^i e_A^j J_{ij} \approx C_+^2 J_+, \quad C_+^2 = \sum_{\nu} (C_V^2 + C_A^2), \quad (15)$$

$$\begin{aligned} J_+ = & \frac{4K^2}{uv} q^2 [2(\mathbf{e}_A \mathbf{p})(\mathbf{e}_A \mathbf{p}') + \varepsilon \varepsilon' - \mathbf{p} \mathbf{p}'] + 8K^2 \\ & - \frac{4K^2}{uv} (\varepsilon \varepsilon' - \mathbf{p} \mathbf{p}') [K^2 - 2(\mathbf{e}_A \mathbf{k})^2] \\ & + 4K^2 \frac{(\mathbf{q} \mathbf{k})^2}{uv} + 4K^4 \frac{(\mathbf{e}_A \mathbf{k})^2}{uv} \\ & - 2K^4 [2(\mathbf{e}_A \mathbf{p})(\mathbf{e}_A \mathbf{p}') + \varepsilon \varepsilon' - \mathbf{p} \mathbf{p}'] \left(\frac{1}{u} - \frac{1}{v} \right)^2 \\ & - \frac{8K^2}{uv} (\mathbf{q} \mathbf{k})(\mathbf{e}_A \mathbf{k})^2 \\ & + K^4 \left(\frac{1}{u^2} + \frac{1}{v^2} \right) (2\mathbf{q} \mathbf{k} - K^2) \\ & - 4K^4 (\mathbf{e}_A \mathbf{k}) \left(\frac{\mathbf{e}_A \mathbf{p}}{u^2} - \frac{\mathbf{e}_A \mathbf{p}'}{v^2} \right), \end{aligned} \quad (16)$$

where we introduce the notations

$$\begin{aligned} u &= \frac{1}{2} (P' + K)^2 = P'K + \frac{1}{2} K^2, \\ v &= -\frac{1}{2} (P - K)^2 = PK - \frac{1}{2} K^2. \end{aligned} \quad (17)$$

Using Eqs. (12), (15), and (16), we get

$$\begin{aligned} Q_{\text{flux}} &= \frac{G_F^2 e^2 C_+^2}{12 (2\pi)^9} \mathcal{A}_F \int \mathbf{d} \mathbf{p} \int \mathbf{d} \mathbf{p}' \int \mathbf{d} \mathbf{k} \delta(p_z - p'_z - k_z) \\ &\times \left(\frac{B(q)}{q} \right)^2 \frac{\omega}{\varepsilon \varepsilon'} J_+ f(1 - f'). \end{aligned} \quad (18)$$

For practical applications, it is convenient to express Q_{flux} in the form

$$\begin{aligned} Q_{\text{flux}} &= \frac{G_F^2 e^2 \phi_0^2 C_+^2}{2268 \hbar^9 c^8} (k_B T)^6 q_0 \mathcal{A}_F L \\ &\approx 2.66 \times 10^{16} \bar{B}_{13} T_9^6 \left(\frac{n_p m_p}{n_0 m_p^*} \right)^{1/2} \\ &\times \left[1 - \left(\frac{T}{T_{cp}} \right)^4 \right]^{1/2} L \quad \text{erg s}^{-1} \text{cm}^{-3}. \end{aligned} \quad (19)$$

Here, $n_0 = 0.16 \text{ fm}^{-3}$ is the standard (nuclear) number density, T_9 is temperature in the units of 10^9 K , and \bar{B}_{13} is defined in Sect. 2. Numerical expression for Q_{flux} takes into account emission of ν_e, ν_μ, ν_τ , so that $C_+^2 \approx 1.675$. In Eq. (19), we introduced

the dimensionless quantity L , defined by

$$\begin{aligned} L &= \frac{189}{(2\pi)^9 T^6 q_0} \int \mathbf{d} \mathbf{p} \mathbf{d} \mathbf{p}' \mathbf{d} \mathbf{k} \delta(p_z - p'_z - k_z) \\ &\times \left(\frac{B(q)}{q \phi_0} \right)^2 \frac{\omega}{\varepsilon \varepsilon'} J_+ f(1 - f'), \end{aligned} \quad (20)$$

with J_+ given by Eq. (16). Notice that Eq. (20) is valid for any axially symmetric distribution of the fluxoid magnetic field $B(r)$ although we will use a specific distribution, Eqs. (3) and (14). An analogous quantity L was introduced in the case of the neutrino-pair bremsstrahlung due to the electron-nucleus scattering. In that case, it had a meaning of the Coulomb logarithm (Haensel et al. 1996).

4. Practical evaluation of L

Let us calculate L from Eq. (20). Since the electrons are strongly degenerate (Sect. 2), the main contribution to L comes from those electron transitions, in which the electron momenta \mathbf{p} and \mathbf{p}' lie in the narrow thermal shell around the Fermi surface, $|\varepsilon - \mu| \lesssim T$ and $|\varepsilon' - \mu| \lesssim T$. In Eq. (20) we may set $\mathbf{d} \mathbf{p} = \varepsilon^2 \mathbf{d} \varepsilon \mathbf{d} \Omega$, where $\mathbf{d} \Omega$ is a solid angle element in the direction of \mathbf{p} . We also put $\varepsilon = p$ since the electrons are ultrarelativistic (Sect. 2). Then we can set $\varepsilon = p_{\text{Fe}}$ in all smooth functions of ε . Afterwards, the integration over ε is standard:

$$\int \mathbf{d} \varepsilon f(1 - f') = \frac{\omega}{e^{\omega/T} - 1}. \quad (21)$$

The integrand in Eq. (20) depends obviously on the relative azimuthal positions of \mathbf{p} , \mathbf{p}' and \mathbf{k} . Thus we can place \mathbf{p} in the (xz) -plane without any loss of generality.

We shall mainly consider the case of $q_0 \ll p_{\text{Fe}}$ typical for the NS cores (Sect. 2). It is convenient to replace the integration over \mathbf{p}' in Eq. (20) by the integration over \mathbf{q} . The integration is simplified because the main contribution comes from the values of $q \ll p_{\text{Fe}}$. Thus we can use the approximation of small-angle scattering. Since k can be comparable to q , we should keep two first terms in Eq. (16). Using the inequalities $k \ll p$ and $q \ll p$ we obtain

$$J_+ \approx 8(\omega^2 - \mathbf{k}^2) \left[\frac{q^2 (\mathbf{e}_A \mathbf{p})^2}{q_r^2 p^2} + 1 \right], \quad (22)$$

where we have neglected the quantity $\varepsilon \varepsilon' - \mathbf{p} \mathbf{p}' = [(\mathbf{q} + \mathbf{k})^2 - \omega^2]/2$ in the first term of (16), and have used the approximate expressions $u \approx v \approx pq_r$, which follow from Eqs. (17). The subscript r denotes the vector component along \mathbf{p} ; $q_r = q_x \sin \theta$, where θ is an angle between \mathbf{p} and the z -axis (electron pitch-angle).

Using energy—momentum conservation, in analogy with the results of Haensel et al. (1996) we obtain

$$\begin{aligned} \omega &= \varepsilon - \varepsilon' \approx q_r + k_r, \\ K^2 &= \omega^2 - k_r^2 - k_t^2 \approx k_0^2 - k_t^2, \\ k_0^2 &= q_r(2\omega - q_r), \\ J_+ &= 8(\omega^2 - \mathbf{k}^2) \frac{q^2}{q_r^2} \sin^2 \theta, \end{aligned} \quad (23)$$

where k_t is a component of \mathbf{k} transverse to \mathbf{p} .

The condition $\omega^2 \geq \mathbf{k}^2$ requires $q_r > 0$, $\omega > q_r/2$ and $k_t^2 < k_0^2 = q_r(2\omega - q_r)$. Taking into account Eq. (21), we obtain

$$L = \frac{189}{2^4 \pi^7 T^6 q_0} \int_0^\pi d\theta \sin^3 \theta \int_0^\infty dq_x \int_{-\infty}^\infty dq_y \left(\frac{B(q)}{\phi_0 q_r} \right)^2 \times \int_{q_r/2}^\infty d\omega \frac{\omega^2}{e^{\omega/T} - 1} \int_0^{k_0} dk_t k_t (k_0^2 - k_t^2). \quad (24)$$

The integrals converge rapidly due to sharp decrease of $B(q)$, Eq. (14). In view of this, we could extend the integration over q_x and q_y up to ∞ , and the lower integration limit over q_y down to $-\infty$.

Integrating over k_t , we have

$$L = \frac{189}{8\pi^7 T^6 q_0} \int_0^\pi d\theta \sin^3 \theta \int_0^\infty dq_x \int_0^\infty dq_y \times \left(\frac{B(q)}{\phi_0} \right)^2 \int_{q_r/2}^\infty d\omega \left(\omega - \frac{q_r}{2} \right)^2 \frac{\omega^2}{e^{\omega/T} - 1}, \quad (25)$$

which can be transformed as

$$L = \frac{189 q_0^3}{32\pi^6 T^6} \int_0^\pi d\theta \sin^3 \theta \int_0^\infty \frac{dq_x}{(q_x^2 + q_0^2)^{3/2}} \times \int_{q_r/2}^\infty d\omega \left(\omega - \frac{q_r}{2} \right)^2 \frac{\omega^2}{e^{\omega/T} - 1}. \quad (26)$$

These equations take into account weak inelasticity of the ef scattering, in analogy with the neutrino bremsstrahlung due to the electron–nucleus collisions (Haensel et al. 1996).

As can be seen from Eq. (26), L depends on the dimensionless parameter $t_0 = T/T_0$:

$$t_0 \approx 0.00786 T_9 \left(\frac{m_p^* n_0}{m_p n_p} \right)^{1/2} \left[1 - \left(\frac{T}{T_{cp}} \right)^4 \right]^{-1/2}, \quad (27)$$

where $T_0 = T_p \sqrt{1 - (T/T_{cp})^4}$, and $T_p = \hbar \omega_p / k_B$ is the proton plasma temperature corresponding to the proton plasma frequency ω_p (Sect. 2). Typically, $T_p \sim 1$ MeV, under the conditions in the NS cores. Let us analyze two extreme cases: $T \ll T_0$ and $T \gg T_0$.

4.1. Low-temperature, bremsstrahlung regime, $T \ll T_0$

In the limiting case of $t_0 \ll 1$, Eq. (26) gives $L = \pi/4$. Then the neutrino emissivity is given by

$$Q_{\text{flux}} = \frac{\pi G_F^2 e^2 \phi_0^2 C_+^2}{9072 \hbar^9 c^8} (k_B T)^6 q_0 \mathcal{A}_F \approx 2.09 \times 10^{16} \bar{B}_{13} T_9^6 \left(\frac{n_p m_p}{n_0 m_p^*} \right)^{1/2} \times \left[1 - \left(\frac{T}{T_{cp}} \right)^4 \right]^{1/2} \text{ erg s}^{-1} \text{ cm}^{-3}. \quad (28)$$

The neutrino emission in the low-temperature regime is very similar to that due to the electron–nucleus bremsstrahlung (e.g., Haensel et al. 1996). In particular, the emissivity Q_{flux} is proportional to T^6 . Therefore we will call this regime the *bremsstrahlung regime*.

For the sake of completeness, we have also examined a not too realistic case of $q_0 \sim p_{Fe}$ at $T \ll T_0$. The analysis is based on Eq. (20). In this case, the integration can be simplified, and reduces to

$$L = \int_0^1 dy \frac{y_0^3}{(y^2 + y_0^2)^2} \frac{1 + y^2}{1 - y^2} \left[1 + \frac{2y^2}{1 - y^2} \log(y) \right], \quad (29)$$

where $y = q/(2p_{Fe})$. Now, L is a function of the only dimensionless parameter (see Sect. 2)

$$y_0 \equiv \frac{\hbar q_0}{2p_{Fe}} = \left(\frac{e^2}{3\pi \hbar c} \frac{p_{Fe}}{m_p^* c} \right)^{1/2} \left[1 - \left(\frac{T}{T_{cp}} \right)^4 \right]^{1/2} \approx 0.0165 \left(\frac{m_p}{m_p^*} \right)^{1/2} \left(\frac{n_e}{n_0} \right)^{1/6} \left[1 - \left(\frac{T}{T_{cp}} \right)^4 \right]^{1/2}. \quad (30)$$

In the limit of $y_0 \ll 1$ we reproduce our basic result $L = \pi/4$. For a finite y_0 , the function L given by Eq. (29) can be fitted (with relative error $< 2.4\%$) by a simple expression

$$L = \frac{\pi}{4\sqrt{1 + 0.7057 y_0^2}}. \quad (31)$$

4.2. High-temperature, synchrotron regime, $T \gg T_0$

In the case of $t_0 \gg 1$, from Eq. (26) we obtain an asymptotic form $L \approx (189/\pi^6) \zeta(5)/t_0$, where $\zeta(5) \approx 1.037$ is the value of the Riemann zeta-function. This yields

$$Q_{\text{flux}} = \frac{\zeta(5) G_F^2 e^2 \phi_0^2 C_+^2}{12\pi^6 \hbar^8 c^7} q_0^2 (k_B T)^5 \mathcal{A}_F \approx 6.89 \times 10^{17} \bar{B}_{13} \times T_9^5 \frac{n_p m_p}{n_0 m_p^*} \left[1 - \left(\frac{T}{T_{cp}} \right)^4 \right] \text{ erg s}^{-1} \text{ cm}^{-3}. \quad (32)$$

The temperature dependence ($Q \propto T^5$) is the same as for the synchrotron emission of neutrinos by electrons (e.g., Kaminker et al. 1991). Thus we will refer to the high-temperature regime as the *synchrotron regime*.

Let us compare the ef -scattering emissivity (32) with the emissivity Q_{syn} of the “purely synchrotron process” for the most important case of $\omega_B^* \ll T \ll \mu^3 \omega_B^*$ (μ_e is the electron chemical potential and $\omega_B^* = eBc/\mu_e$ is the electron gyrofrequency). For the uniform magnetic field Kaminker et al. (1991) obtained:

$$Q_{\text{syn}} = \frac{2\zeta(5)}{9\pi^5} \frac{e^2 G_F^2 C_+^2 (k_B T)^5 B^2}{\hbar^8 c^7} \approx 9.04 \times 10^{14} B_{13}^2 T_9^5 \text{ ergs cm}^{-3} \text{ s}^{-1}. \quad (33)$$

(The numerical factor 9.04 differs from a factor 8.97 in Eq. (17) of Kaminker et al. 1991, because in the present paper we use more accurate value of the Fermi constant G_F .)

We start with a brief discussion of the ef scattering at $t_0 \gg 1$ for an arbitrary distribution of the fluxoid magnetic field $B(q)$. In this case, we can set $q_r \rightarrow 0$ in Eq. (25). Then the integrations over θ and ω are decoupled from the integration over \mathbf{q} , and can be done analytically. This yields the emissivity

$$Q_{\text{flux}} = \frac{1}{12\pi^7} \zeta(5) G_F^2 C_+^2 T^5 \mathcal{A}_F \int d\mathbf{q} B^2(q), \quad (34)$$

where the integration should be done over the entire (q_x, q_y) plane. The emissivity is seen to be independent of the electron Fermi momentum. In particular, in the limit of a (quasi) uniform magnetic field $B(r) = B_0$, $B(q) = 4\pi^2 B_0 \delta^{(2)}(\mathbf{q})$, we can replace $B(q)^2 \rightarrow 4\pi^2 B_0^2 \delta^{(2)}(\mathbf{q})/\mathcal{A}_F$, and obtain

$$Q_{\text{flux}} = \frac{\zeta(5)}{3\pi^5} \frac{e^2 G_F^2 C_+^2 (k_B T)^5 B_0^2}{\hbar^8 c^7}. \quad (35)$$

Comparing (35) and (33), we have $Q_{\text{syn}} = (2/3) Q_{\text{flux}}$. The same factor $2/3$ is obtained, if we treat B in Q_{syn} as a local magnetic field of a fluxoid, average $Q_{\text{syn}} \propto B^2$ over a lattice of fluxoids with the magnetic field (3), and compare the result with Q_{flux} , Eq. (32). Let us emphasize, that this emissivity \bar{Q}_{syn} , averaged over a nonuniform magnetic field, can differ from the synchrotron emissivity Q_{syn} in the initial uniform field \bar{B} by a large factor of $B^2/\bar{B}^2 = \phi_0 q_0^2/(4\pi\bar{B}) \sim (d_F/\lambda)^2$, where d_F is an inter-fluxoid distance (Sect. 2). This increase of \bar{Q}_{syn} is caused by the magnetic field enhancement within the fluxoids due to magnetic flux conservation. The enhancement is much stronger than the reduction of neutrino-emission space occupied by the fluxoids.

A detailed analysis shows, that the difference by a factor of $2/3$ comes from momentum space available for neutrino-pair momentum \mathbf{k} . The space is different in the case of synchrotron radiation in a *uniform magnetic field* and in the case of ef scattering by *magnetic inhomogeneities* (in our case — fluxoids). Let us fix the electron pitch angle θ and average over the electron Larmor rotation. In the both cases \mathbf{k} is concentrated to the cone of a given θ (neutrinos are emitted predominantly within a narrow angle interval $\delta\theta$ in the direction of the electron pitch angle θ), and typically, $k \sim T$. In the case of the ef scattering, our estimates yield $\delta\theta_{\text{flux}} \sim \sqrt{q_0/T}$. The synchrotron radiation consists of many discrete cyclotron harmonics s with typical values $s \sim T/\omega_B^* \gg 1$, for the quasiclassical regime of interest. For a fixed θ , the radiation in each harmonics is peaked at the pitch-angle cone, and maximum neutrino momenta \mathbf{k} are restricted by a parabolic surface (Kaminker et al. 1991). The maximum value of k in the pitch-angle direction is $s\omega_B^*/(\sin\theta)^2$, and, typically, $\delta\theta_{\text{syn}} \sim s^{-1/3}$. Replacing a sum over harmonics by an integral we obtain a smoothed synchrotron \mathbf{k} space. It fills only $2/3$ of the available momentum space, due to the *parabolic momentum space restriction* for each harmonics (e.g., the surface area below the parabolic curve $y = 1 - x^2$ at $0 \leq x \leq 1$ is exactly $2/3$ of the surface area below a straight segment $y = 1$). A transition from the synchrotron formula (33) to the fluxoid formula (32) is expected to occur at $\delta\theta_{\text{flux}} \sim \delta\theta_{\text{syn}}$. This is equivalent to the condition $\lambda \sim (c/\omega_B^*)s^{-1/3}$, which takes place when the scale of

the magnetic field variation λ becomes comparable to a distance along which a neutrino pair is emitted in a uniform magnetic field, i.e., to the $s^{1/3}$ -th part of the Larmor radius c/ω_B^* .

4.3. Overall fit and overview

Combining the results of Sects. 4.1 and 4.2, we can propose the following fitting expression for the quantity L in Eq. (19) at $y_0 \ll 1$:

$$L = L_0 U V, \quad (36)$$

$$L_0 = \frac{\pi}{4} \frac{0.260 t_0 + 0.0133}{t_0^2 + 0.25 t_0 + 0.0133}, \quad U = \frac{2\gamma + 1}{3\gamma + 1},$$

$$\gamma = \left(\frac{\hbar\omega_B^*}{\mu_e} \right)^2 \frac{t_0}{y_0^2} \approx 8.38 \times 10^{-12} T_9 \bar{B}_{13}^2$$

$$\times \left(\frac{n_0}{n_e} \right)^{13/6} \left(\frac{m_p^*}{m_p} \right)^{3/2} \left[1 - \left(\frac{T}{T_{cp}} \right)^4 \right]^{-3/2}. \quad (37)$$

$$V = 1 + \frac{4\pi\bar{B}\lambda^2}{\phi_0}$$

$$\approx 1 + 0.00210 \bar{B}_{13} \frac{m_p^* n_0}{m_p n_p} \left[1 - \left(\frac{T}{T_{cp}} \right)^4 \right]^{-1}. \quad (38)$$

Here, L_0 is the analytic expression which fits the results of our numerical calculations of L from Eq. (26) with error $< 1\%$ for any t_0 . The factor U ensures, somewhat arbitrarily, the difference by a factor of $2/3$ between the cases of weakly and strongly nonuniform magnetic fields (Sect. 4.2). The factor V provides a smooth transition from the ef scattering to the pure synchrotron emission in the case when a fluxoid radius λ becomes very large ($T \rightarrow T_{cp}$), the neighboring fluxoids overlap and the overall magnetic field becomes nearly uniform.

Using our results, we can follow the evolution of Q_{flux} in the course of the superconductivity onset. If $T \geq T_{cp}$, the emissivity Q_{flux} is given by Eq. (33) since it is essentially the same as the synchrotron emissivity $Q_{\text{syn}}^{(0)} = Q_{\text{syn}}(\bar{B})$ in a locally uniform ‘primordial’ magnetic field $B = \bar{B}$. After T falls only slightly below T_{cp} , the factor U transforms from $U = 2/3$ (‘pure synchrotron’) to $U = 1$ (ef scattering in the synchrotron regime). The fluxoid structure is still not very pronounced, i.e., $V \approx 4\pi\bar{B}\lambda^2/\phi_0$, $Q_{\text{flux}} \sim Q_{\text{syn}}^{(0)}$. When T decreases to about $0.8 T_{cp}$, the fluxoid radius λ nearly achieves its zero-temperature value λ_0 , and $V \simeq 1$. Accordingly, $Q_{\text{flux}}/Q_{\text{syn}}^{(0)}$ grows by a factor of $(d_F/\lambda_0)^2$ due to the magnetic field confinement within the fluxoids (Sect. 4.2). Simultaneously, t_0 decreases from very large values at $T \rightarrow T_{cp}$ to $t_0 \simeq T_{cp}/T_p$.

Let us first consider the case in which the proton plasma temperature is $T_p \ll T_{cp}$. Then the emissivity Q_{flux} is enhanced with respect to $Q_{\text{syn}}^{(0)}$ by a factor of $(d_F/\lambda_0)^2$ at $T \approx 0.8 T_{cp}$, and this enhancement remains nearly constant over a wide temperature range down to T_p . Within this range, the ef scattering operates in the synchrotron regime. At lower temperatures, $T \lesssim T_p$, the synchrotron regime transforms into the bremsstrahlung regime

(Sect. 4.1) and we have $Q_{\text{flux}} \sim Q_{\text{syn}}^{(0)} (d_F/\lambda_0)^2 (T/T_p)$. Thus, for $T \lesssim T_p$ the emissivity Q_{flux} decreases with respect to $Q_{\text{syn}}^{(0)}$, and may become lower than $Q_{\text{syn}}^{(0)}$.

In the opposite case of $T_p \gtrsim T_{cp}$, the ef scattering operates in the synchrotron regime only in a narrow temperature range below T_{cp} , and transforms into the bremsstrahlung regime at lower T . In the latter regime, we have $Q_{\text{flux}} \sim Q_{\text{syn}}^{(0)} (d_F/\lambda)^2 (T/T_p)$.

5. Neutrino bremsstrahlung due to ep and ee scattering

As will be shown in Sect. 6, the ef scattering mechanism can be important, if protons and neutrons in a NS core are highly superfluid (have high critical temperatures T_{cp} , T_{cn}), so that the rates of the ‘‘standard’’ Urca and nucleon bremsstrahlung processes are strongly suppressed. Under such conditions, one should carefully take into account *all* the neutrino processes, even if they are negligible for relatively low critical temperatures.

In this section, we consider two additional neutrino production mechanisms, the neutrino-pair bremsstrahlung due to the ep and ee scattering:

$$\begin{aligned} e + p &\rightarrow e + p + \nu + \bar{\nu}, \\ e + e &\rightarrow e + e + \nu + \bar{\nu}. \end{aligned} \quad (39)$$

As far as we know, these mechanisms were neglected in the neutron-star cooling simulations.

Let us restrict ourselves to simple estimates of the emissivities Q_{ep} and Q_{ee} ; detailed analysis will be published elsewhere (Kaminker et al. in preparation). We start from the well-known emissivity Q_{eZ} of the electron-nucleus bremsstrahlung (e.g., Haensel et al. 1996). In the particular case of the ep collisions of relativistic, strongly degenerate electrons in a nonsuperfluid matter, we obtain

$$Q_{ep}^{(0)} = \frac{8\pi C_+^2 e^4 G_F^2}{567 \hbar^9 c^8} (k_B T)^6 n_p L_{ep}, \quad (40)$$

where L_{ep} is the Coulomb logarithm. The above formula has been derived assuming, that an energy transfer to a proton in a neutrino-emission act is much smaller than T . As applied to our case of strongly degenerate protons, the latter means that the Pauli principle imposes no restrictions on the states of protons. This is true as long as $T \gg q_s$, where q_s is an inverse length of plasma screening of the Coulomb ep interaction (see below). However, in reality we have just an opposite regime, $T \ll q_s$, and Eq. (40) does not hold.

To estimate Q_{ep} at $T \ll q_s$, we assume that $Q_{ep} \propto \nu_{ep}$, where ν_{ep} is some effective ep collision frequency. If our assumption is correct, we have $Q_{ep} \approx Q_{ep}^{(0)} \nu_{ep}/\nu_{ep}^{(0)}$, where $\nu_{ep}^{(0)}$ and ν_{ep} refer to the high- and low- temperature cases, respectively. For high temperatures, we will use the effective frequency of nearly elastic collisions $\nu_{ep}^{(0)}$ (e.g., Yakovlev and Urpin 1980) which determines the electric and thermal conductivities of degenerate electrons. For $T \ll q_s$, we employ the collision frequency ν_{ep} that determines the electron thermal conductivity

(e.g., Gnedin and Yakovlev 1995). Performing the above rescaling, we obtain

$$\begin{aligned} Q_{ep} &= \frac{\pi^5 G_F^2 e^4 C_+^2 m_p^{*2}}{945 \hbar^9 c^8 y_s^3 p_{Fe}^4} n_p (k_B T)^8 R_{ep} \\ &\approx \frac{3.42 \times 10^{14}}{y_s^3} \left(\frac{m_p^*}{m_p} \right)^2 \left(\frac{n_0}{n_p} \right)^{1/3} \\ &\times R_{ep} T_9^8 \text{ ergs cm}^{-3} \text{ s}^{-1}, \end{aligned} \quad (41)$$

where $y_s = \hbar q_s/(2p_{Fe})$ is the plasma screening parameter. We additionally introduce the factor R_{ep} that describes suppression of the emissivity by the proton superfluidity. According to Gnedin & Yakovlev (1995) the plasma screening in npe matter of the NS cores is defined by

$$y_s^2 = \frac{e^2}{\pi \hbar c} \left(1 + \frac{m_p^* p_{FP}}{m_e^* p_{Fe}} Z_p \right), \quad (42)$$

where $m_e^* = \mu_e/c^2$. The first term in brackets comes from the electron screening while the second is due to the proton screening. The latter contains the factor Z_p which describes reduction of the proton screening by the proton superfluidity. According to Gnedin & Yakovlev (1995) this factor is fitted as

$$\begin{aligned} Z_p &= \left(0.9443 + \sqrt{(0.0557)^2 + (0.1886v)^2} \right)^{1/2} \\ &\times \exp \left(1.753 - \sqrt{(1.753)^2 + v^2} \right), \end{aligned} \quad (43)$$

where v is the proton superfluid gap parameter

$$\begin{aligned} v &= \frac{\Delta_p(T)}{k_B T} = \sqrt{1 - \frac{T}{T_{cp}}} \\ &\times \left(1.456 - 0.157 \sqrt{\frac{T_{cp}}{T}} + 1.764 \frac{T_{cp}}{T} \right). \end{aligned} \quad (44)$$

If protons are normal ($T \geq T_{cp}$), one has $R_{ep} = Z_p = 1$ in Eqs. (41) and (42). The factor R_{ep} , which damps Q_{ep} at $T < T_{cp}$, should be the same as the factor R_{np} that describes reduction of the neutrino emission in np collisions by the proton superfluidity (Yakovlev and Levenfish 1995):

$$\begin{aligned} R_{ep} &= \frac{1}{2.732} \left[a \exp \left(1.306 - \sqrt{(1.306)^2 + v^2} \right) \right. \\ &\left. + 1.732 b^7 \exp \left(3.303 - \sqrt{(3.303)^2 + 4v^2} \right) \right], \end{aligned} \quad (45)$$

with $a = 0.9982 + \sqrt{(0.0018)^2 + (0.3815v)^2}$,
 $b = 0.3949 + \sqrt{(0.6051)^2 + (0.2666v)^2}$.

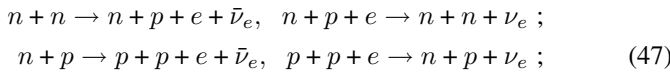
Now consider the neutrino emissivity Q_{ee} due to ee scattering. Under the same assumption, we obtain $Q_{ee} = Q_{ep} \nu_{ee}/\nu_{ep}$, where ν_{ee} is the effective ee collision frequency that determines the electron thermal conductivity (e.g., Gnedin & Yakovlev 1995). Then

$$\begin{aligned} Q_{ee} &= \frac{\pi^5 G_F^2 e^4 C_+^2}{378 \hbar^9 c^{10} y_s^3 p_{Fe}^2} n_e (k_B T)^8 \\ &\approx \frac{1.07 \times 10^{14}}{y_s^3} \left(\frac{n_e}{n_0} \right)^{1/3} T_9^8 \text{ ergs cm}^{-3} \text{ s}^{-1}. \end{aligned} \quad (46)$$

Although we do not calculate Q_{pe} and Q_{ee} exactly, we believe that Eqs. (41) and (46) give reliable estimates. The emissivity Q_{ep} is reduced exponentially by the strong proton superfluidity, while Q_{ee} is affected by the superfluidity in a much weaker manner, only through the plasma screening parameter (42). If protons are normal they provide the major contribution into the plasma screening. If they are strongly superfluid, a weaker electron screening becomes important, which *enhances* Q_{ee} , but not to a great extent (see below).

6. Discussion

Figs. 1 and 2 illustrate the efficiency of various neutrino production mechanisms in npe matter of the NS cores. We compare the neutrino emissivity due to the ef scattering or due to the electron synchrotron radiation (Sect. 4) with those produced by the neutron and proton branches of the modified Urca reactions (Friman & Maxwell 1979, Yakovlev & Levenfish 1995),



by the nucleon-nucleon bremsstrahlung processes (Friman & Maxwell 1979, Yakovlev & Levenfish 1995)



and also by the ep and ee bremsstrahlung processes (39) considered in Sect. 5. For better presentation, the total emissivity of the both branches of the modified Urca reactions (47) is represented by a single curve ‘*Murca*’, and the total emissivity from the three nucleon-nucleon bremsstrahlung reactions (48) are represented by a single curve ‘*NN*’. We adopted a moderately stiff equation of state of Prakash et al. (1988) (the same version as used by Page & Applegate 1992) and choose matter density $\rho = 5.6 \times 10^{14} \text{ g cm}^{-3}$ ($n_p = n_e \approx 0.0207 \text{ fm}^{-3}$, $n_n \approx 0.323 \text{ fm}^{-3}$), well below the threshold density $1.30 \times 10^{15} \text{ g cm}^{-3}$ at which the direct Urca process becomes allowed (Lattimer et al. 1991). Therefore our curves correspond to the *standard* neutrino emission (no exotic cooling agents, see, e.g., Pethick 1992). We show temperature dependence of various neutrino emissivities in the range from 10^8 K to $5 \times 10^9 \text{ K}$, which is the most important for the cooling theories of NS. The nucleon effective masses are set equal to 0.7 of the masses of bare particles. The neutrino emissivities vary slowly with density (below the direct Urca threshold), i.e., we present a typical situation within the NS cores. In both figures, we assume the presence of the ‘primordial’ magnetic field $\bar{B} = 10^{12}$, 10^{13} or 10^{14} G .

Fig. 1 corresponds to a nonsuperfluid matter. If the magnetic field is absent, the *Murca* processes are seen to be the most important ones, in the displayed temperature range. The *NN* bremsstrahlung is much weaker, and the ep and ee bremsstrahlung processes are even weaker. The emissivities of all these mechanisms vary as T^8 , whereas the emissivity of

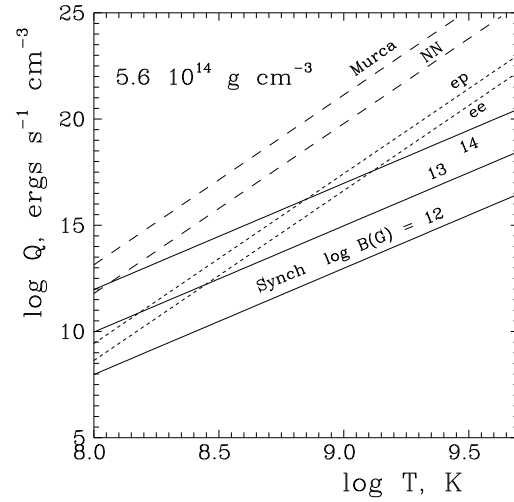


Fig. 1. Neutrino energy loss rates from various processes, versus temperature in a non-superfluid npe matter of density $5.6 \times 10^{14} \text{ g cm}^{-3}$. *Murca* — total contribution of two branches of the modified Urca process, Eq. (47); *NN* — total contribution of three nucleon bremsstrahlung processes, Eq. (48); *ep* and *ee* — bremsstrahlung processes, Eq. (39), due to the ep and ee scattering, respectively; solid lines — synchrotron radiation of electrons for three values of the magnetic field.

the synchrotron radiation varies as T^5 . Thus the synchrotron radiation is negligible for $T \gtrsim 10^9 \text{ K}$ but becomes more important with decreasing T . At $T \sim 10^8 \text{ K}$ and $B = 10^{14} \text{ G}$ the synchrotron dominates over all other mechanisms except the *Murca* processes, and at slightly lower T it becomes the most efficient of all mechanisms. However, such temperatures are too low to be important for the cooling theories: the neutrino luminosity of NS becomes then smaller than the photon luminosity from the stellar surface, and the neutrino emission loses its significance as a source of the NS cooling. Fig. 2 shows how the neutrino emission displayed in Fig. 1 is modified by the nucleon superfluidity. In our example, the protons and neutrons become superfluid at $T_{cp} = T_{cn} = 2 \times 10^9 \text{ K}$. These are typical, moderate critical temperatures for the nucleon superfluidity (e.g., Takatsuka & Tamagaki 1993). The factors which describe superfluid suppression of the modified Urca processes (47) and *NN* collisions (48) are taken from Yakovlev & Levenfish (1995). At $T \lesssim 10^9 \text{ K}$ the nucleon superfluidity is seen to strongly reduce all the neutrino production processes which involve nucleons. If the magnetic field were absent, the ee scattering would be the main neutrino generation mechanism at $T \lesssim 5 \times 10^8 \text{ K}$. However, the ef scattering in the presence of $\bar{B} \gtrsim 10^{13} \text{ G}$ also becomes important, and it can even dominate. After the superfluidity onset ($T < T_{cp}$), the magnetic field splits into fluxoids and the synchrotron radiation transforms into the radiation due to the ef scattering. This enhances Q_{flux} owing to the field amplification within the fluxoids (Sect. 4). The enhancement is more pronounced at lower $\bar{B} \sim 10^{12} \text{ G}$ at which the field amplification is stronger. This is a rare case in which the neutrino emissivity *increases* with decreasing T . For the

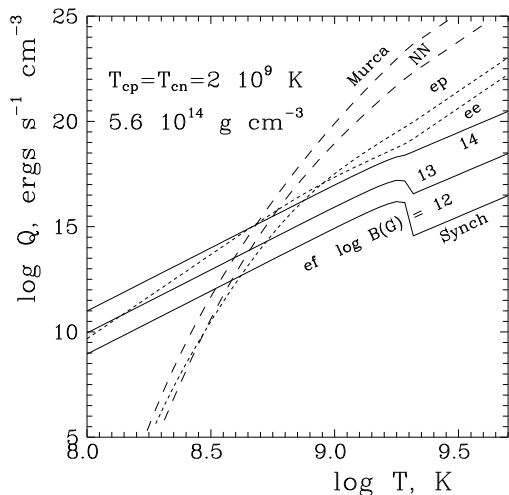


Fig. 2. Same as in Fig. 1 but in the presence of proton and neutron superfluidities with $T_{cp} = T_{cn} = 2 \times 10^9$ K. At $T < T_{cp}$ the initially uniform magnetic field splits into fluxoids, and the synchrotron emission transforms into the emission due to the ef scattering. The nucleon superfluidity suppresses all mechanisms but the ee and ef scattering.

conditions displayed in Fig. 2, the proton plasma temperature $T_p = 5.47 \times 10^{10}$ K is much higher than the superfluid critical temperature T_{cp} . Therefore, the synchrotron regime (Sect. 4.2) in the ef scattering operates only at $T \lesssim T_{cp}$, during the phase of the fluxoid formation. Very soon after T falls below T_{cp} , the synchrotron regime transforms into the bremsstrahlung regime (Sect. 4.1) which operates further with decreasing T .

We have analysed a number of cases, varying the proton and neutron critical temperatures T_{cp} and T_{cn} . Our principal conclusion is that the standard neutrino production mechanisms (47) and (48) dominate in the temperature domain of practical interest if either T_{cp} and/or T_{cn} are not too high (not higher than about 10^9 K). If, however, both critical temperatures are high, the situation is similar to that shown in Fig. 2. The superfluidity suppresses all the traditional neutrino generation mechanisms, and the main neutrino production at $T \lesssim 5 \times 10^8$ K comes either from the ef or the ee scattering.

In principle, neutrinos can be generated also in the pp collisions of *normal* protons in the non-superfluid cores of the fluxoids (Sect. 2) as well as in the en collisions. However, the non-superfluid cores are very thin, the emission volume is minor, and the first process is inefficient. The neutrino bremsstrahlung due to en scattering is also inefficient since it occurs through electromagnetic interaction involving neutron magnetic moment (e.g., Baym et al. 1969) and since it is suppressed by the neutron superfluidity.

While it is commonly accepted that protons form a type II superconductor, a possibility that they actually form a type I superconductor cannot be excluded. This uncertainty results from the lack of a precise knowledge of the nucleon-nucleon interaction in dense nuclear matter, and from the approximations and deficiencies of the many-body theory of dense nucleon matter.

In the case of a type I proton superconductor, which corresponds to $\xi_0 > \sqrt{2}\lambda_0$ (de Gennes 1966), cooling below T_{cp} is expected to be accompanied by a transition of the magnetized interior to an “intermediate state” (de Gennes 1966, Baym et al. 1969). The “intermediate state” would consist of alternating regions of normal matter containing magnetic flux, and superconducting regions exhibiting a complete expulsion of magnetic flux. The specific spatial structure of the “intermediate state” would result from the condition of the minimum of the thermodynamic potential at a fixed macroscopic magnetic flux (de Gennes 1966). Qualitatively, we expect that the presence of an “intermediate state” in the superconducting proton core will imply an enhancement of its electron synchrotron $\bar{\nu}\nu$ emissivity, compared to the case of a normal proton core, because of $\bar{B}^2 > (\bar{B})^2$. However, for $\bar{B} \lesssim 10^{14}$ G this enhancement will be much smaller than that characteristic of the type II superconductor, in which magnetic field is confined to fluxoids.

7. Conclusion

We have considered (Sects. 3 and 4) the neutrino-pair radiation (4) due to scattering of relativistic, degenerate electrons off threads of quantum magnetic flux — fluxoids — in the npe matter within the superfluid NS cores. We have shown that this mechanism is a natural generalization of the synchrotron emission of neutrinos by electrons in a non-superconducting matter (with a locally uniform magnetic field) to the case in which the protons become superfluid and the magnetic field splits into the fluxoids. According to our results, this mechanism can operate either in the synchrotron (Sect. 4.2) or in the bremsstrahlung (Sect. 4.1) regime. We have obtained a simple fitting expression (36) which reproduces the emissivity (19) for any parameters of practical interest.

Furthermore, we have estimated (Sect. 5) the neutrino emissivities in two additional neutrino production mechanisms (39), the ep and ee bremsstrahlung processes. In a non-superfluid matter, these mechanisms are much weaker than the standard neutrino emission mechanisms, such as the modified Urca processes (47) and the nucleon–nucleon bremsstrahlung (48). If, however, both superfluid critical temperatures, T_{cp} and T_{cn} , are higher than 10^9 K, then the superfluidity strongly suppresses all the traditional (standard) neutrino energy losses. In such a case, the main neutrino generation in a NS core at $T \lesssim 5 \times 10^8$ K occurs either via the electron-fluxoid or via the ee scattering (Sect. 6). Therefore our results can be of particular importance for simulating the cooling of NSs with highly superfluid cores.

Acknowledgements. The authors are grateful to Kseniya Levenfish who participated at the initial stage of this work. One of the authors (ADK) acknowledges excellent working conditions and hospitality of N. Copernicus Astronomical Center in Warsaw. This work was supported in part by the RBRF (grant No. 96-02-16870a), INTAS (grant No. 94-3834), DFG-RBRF (grant No. 96-02-00177G), and the KBN grant 2P 304 014 07.

References

- Baym, G., Pethick, C., Pines, D. 1969, *Nature*, 224, 673
- Berestetskii, V.B., Lifshitz, E.M., Pitaevskii, L.P. 1982, *Quantum Electrodynamics*, Pergamon, Oxford
- Bhattacharya, D., Srinivasan, G. 1995, in: W.H. Lewin, J. van Paradijs, E.P.J. van den Heuvel (eds) *X-Ray Binaries*. Cambridge UP, Cambridge, p. 495
- Festa, G.G., Ruderman, M.A. 1969, *Phys. Rev.*, 180, 1227
- Friman, B.L., Maxwell, O.V. 1979, *ApJ*, 232, 541
- de Gennes, P.G. 1966, *Superconductivity of Metals and Alloys*, Benjamin, New York
- Gnedin, O.Y., Yakovlev, D.G. 1995, *Nucl. Phys.*, A582, 697
- Haensel, P., Kaminker, A.D., Yakovlev, D.G. 1996, *A&A*, 314, 328
- Jones, P.B. 1987, *MNRS*, 228, 513
- Kaminker, A.D., Levenfish, K.P., Yakovlev, D.G. 1991, *Astron. Lett.*, 17, 1090
- Kaminker, A.D., Levenfish, K.P., Yakovlev, D.G., Amsterdamski, P., Haensel, P. 1992, *Phys. Rev.*, D46, 3256
- Lattimer, J.M., Pethick, C.J., Prakash, M., Haensel, P. 1991, *Phys. Rev. Lett.*, 66, 2701
- Lifshitz, E.M., Pitaevskii, L.P. 1980, *Statistical Physics*, part 2, Pergamon, Oxford
- Lorenz, C.P., Ravenhall, D.G., Pethick, C.J. 1993, *Phys. Rev. Lett.*, 70, 379
- Muslimov, A.G., Tsygan, A.I. 1985, *Astrophys. Space Sci.*, 115, 43
- Page, D., Applegate, J.H. 1992, *ApJ (Letters)*, 394, L17
- Pethick, C.J. 1992, *Rev. Mod. Phys.*, 64, 1133
- Prakash, M., Ainsworth, T.L., Lattimer, J.M. 1988, *Phys. Rev. Lett.*, 61, 2518
- Sauls, J.A. 1989, in: H. Ögelman and E.P.J. van den Heuvel (eds) *Timing Neutron Stars*. Dordrecht: Kluwer Academic Publishers, p. 457
- Schaab, C., Weber, F., Weigel, M.K., Glendenning, N.K. 1996, *Nucl. Phys.*, A605, 531
- Soyeur, M., Brown, G.E. 1979, *Nucl. Phys.*, A324, 464
- Srinivasan, G., Bhattacharya, D., Muslimov, A.G., Tsygan, A.I. 1990, *Current Science*, 59, 31
- Takatsuka, T., Tamagaki, R. 1993, *Progr. Theor. Phys. Suppl.*, 112, 27
- Tilley, D.R., Tilley, J. 1990, *Superfluidity and Superconductivity*, Graduate Student Series in Physics. Bristol: IOP Publishing
- Yakovlev, D.G., Levenfish, K.P. 1995, *A&A*, 297, 717
- Yakovlev D.G., Urpin V.A. 1980, *SvA* 24, 303